

## INTERNAL KINEMATICS OF THE ANDROMEDA II DWARF SPHEROIDAL GALAXY

PATRICK CÔTÉ<sup>1,2</sup>, MARIO MATEO<sup>3</sup>, EDWARD W. OLSZEWSKI<sup>4</sup> AND K.H. COOK<sup>5</sup>

*Accepted for publication in the Astrophysical Journal, November 10 1999 issue.*

### ABSTRACT

The High Resolution Echelle Spectrometer on the Keck I telescope has been used to measure nine radial velocities having a median precision of  $\simeq 2$  km s<sup>-1</sup> for seven red giants belonging to the isolated dwarf spheroidal galaxy Andromeda II (And II). We find a weighted mean radial velocity of  $\bar{v}_r = -188 \pm 3$  km s<sup>-1</sup> and a central velocity dispersion of  $\sigma_0 = 9.3_{-2.6}^{+2.7}$  km s<sup>-1</sup>. There may be evidence for a radial velocity gradient across the face of the galaxy, although the significance of this result is low due to the small number of stars having measured velocities. Our best estimate for the global mass-to-light ratio of And II is  $M/L_V = 20.9_{-10.1}^{+13.9} M_\odot/L_{V,\odot}$ . This value is similar to those of several Galactic dwarf spheroidal galaxies and is consistent with the presence of a massive dark halo in And II.

*Subject headings:* galaxies: dwarf — galaxies: kinematics and dynamics — galaxies: individual (Andromeda II)

### 1. INTRODUCTION

The nine dwarf spheroidal (dSph) galaxies belonging to the Milky Way are among the faintest known galaxies in the universe. Studies of their internal kinematics began with the pioneering work of Aaronson (1983), who reported an unexpectedly large internal velocity dispersion of 6.5 km s<sup>-1</sup> for the Draco dSph galaxy: a result based on radial velocities for three carbon stars. Subsequent work has not only confirmed this result but has established that every Galactic dSph galaxy has a central velocity dispersion in the range 6-13 km s<sup>-1</sup> (*e.g.*, Suntzeff et al. 1993; Hargreaves et al. 1994; Vogt et al. 1995; Mateo et al. 1998). These anomalous velocity dispersions constitute the single most compelling piece of evidence that the Galactic dSph galaxies are embedded in massive dark halos.

Long-term monitoring of the radial velocities of red giants belonging to the Galactic dSphs, and the acquisition and analysis of greatly expanded radial velocity samples, suggest that several alternative explanations for the high velocity dispersions of these galaxies — such as binary stars, pulsations in the atmospheres of the most luminous dSph stars and non-isotropic velocity distributions — no longer appear viable (Olszewski, Aaronson & Hill 1996; Hargreaves, Gilmore & Annan 1996; Pryor & Kormendy 1990). The remaining alternatives to the conclusion that dSph galaxies are enveloped in dark halos of mass  $\sim 2 \times 10^7 M_\odot$  (Mateo et al. 1993) are severe heating by the Galactic tidal field (Kuhn & Miller 1989; Klessen & Kroupa 1998; cf. Piatek & Pryor 1995) and/or the possibility that these diffuse galaxies occupy a “low-acceleration regime” in which Newtonian gravity does not strictly apply (Milgrom 1983; 1990). Although all nine Galactic dSphs have now had their internal kinematics studied (albeit in varying levels of detail), it is clear that some fundamental

questions remain unanswered.

As the nearest of the dSph galaxies associated with M31, Andromeda II (And II) is a promising target for a kinematic study. Since this galaxy is relatively isolated (van den Bergh 1972; König et al. 1993), the detection of a high central velocity dispersion would vitiate arguments that the internal motions of Galactic dSphs are dominated by non-equilibrium dynamics. In this *Letter*, we present an analysis of the internal kinematics of And II based on nine radial velocities for seven red giants in And II obtained with the Keck I telescope.

### 2. OBSERVATIONS AND REDUCTIONS

#### 2.1. Object Selection and HIRES Spectroscopy

Red giant members of And II were selected from the study of Côté, Oke & Cohen (1999) who present *VI* photometry and intermediate-resolution spectroscopy for 50 candidate red giants in And II. Echelle spectra for And II member giants were obtained on the nights of 14-15 and 15-16 October 1998 using the High Resolution Echelle Spectrometer (HIRES; Vogt et al. 1994) on the Keck I telescope. The detector was binned 2×2, giving an effective area of 1024×1024 pixels. A single readout amplifier was employed, adjusted to a gain setting of 2.4 e<sup>-1</sup>/ADU. The cross-disperser and grating angles were fixed at -0.05° and 0.0°, respectively. Since the cross disperser was used in first order, these angles yielded a spectral coverage of 4480  $\lesssim \lambda \lesssim$  6900 Å. The entrance aperture was limited to 1'15×7'0 with the C5 decker. Exposure times for all And II stars were 3600s, with Th-Ar comparison lamp spectra taken immediately before and after each exposure. Observing conditions throughout the run were excellent.

The data were reduced in a manner identical to that described in Vogt et al. (1995). A total of 29 separate apertures were extracted for each program object, although af-

<sup>1</sup>California Institute of Technology, Mail Stop 105-24, Pasadena, CA 91125

<sup>2</sup>Sherman M. Fairchild Fellow

<sup>3</sup>Department of Astronomy, 821 Dennison Building, University of Michigan, Ann Arbor, MI 48109

<sup>4</sup>Steward Observatory, University of Arizona, Tucson, AZ 85721

<sup>5</sup>Lawrence Livermore National Laboratory, Livermore, CA 94550

ter some experimentation it was decided to use only eight orders in measuring radial velocities (*i.e.*, those spanning the range  $4848 \lesssim \lambda \lesssim 5413 \text{ \AA}$ ). Eleven high-S/N spectra for seven different IAU radial velocity standard stars were also obtained during the two night run. These spectra were reduced in a similar manner to those of the And II program stars and were used to create a master template as described in Vogt et al. (1995). Radial velocities for And II red giants were then derived by cross-correlating their spectra against that of the master template.

A critical step in deriving mass-to-light ratios from radial velocity measurements is the proper determination of the velocity uncertainties. This is best done empirically, using repeat radial velocity measurements (preferably obtained during separate observing runs). We have combined the 34 velocities of 14 stars given in Vogt et al. (1995) and Mateo et al. (1998) with additional velocities for four stars (including two And II members) obtained during this run. All velocities were obtained using identical instrumental setups and similar reduction procedures using IRAF.<sup>6</sup> We express the velocity uncertainty of each measurement as

$$\sigma_v = \alpha / (1 + R_{TD}), \quad (1)$$

where  $R_{TD}$  is a parameter which measures the height of the cross-correlation peak relative to the local noise in the cross-correlation function, and  $\alpha$  is a constant which must be determined empirically (Tonry & Davis 1979). Based on our sample of repeats, we adopt  $\alpha = 12.0$  which is slightly lower than, but consistent with, the values of 14.9 and 13.4 found by Mateo et al. (1998) and Cook et al. (1999) using smaller samples. It is, however, inconsistent with the value of 26.4 given in Vogt et al. (1995) although the difference is due primarily to a single discrepant star (Leo #23) which was discarded since it was found to contribute nearly half of the total  $\chi^2$  for the sample. We conclude that that equation 1 with  $\alpha = 12.0$  closely reflects our true velocity errors, and refer the reader to Côté et al. (1999a) for a full discussion of the determination of  $\alpha$ .

The results are summarized in Table 1, which gives for each star the ID number,  $V$  magnitude,  $(V - I)$  color, projected galactocentric distance, position angle, heliocentric Julian date and  $R_{TD}$ . The final two columns give the individual and mean heliocentric radial velocities. Finding charts for the program stars may be found in Côté et al. (1999b).

### 3. ANALYSIS

#### 3.1. Mean Velocity, Velocity Dispersion and the Possibility of Rotation

Using the velocities given in Table 1, we find  $\bar{v}_r = -188.1 \pm 2.8 \text{ km s}^{-1}$  and  $\sigma_{mle} = 7.1 \pm 2.1 \text{ km s}^{-1}$  using the Pryor & Meylan (1993) maximum-likelihood estimators for the weighted mean radial velocity and intrinsic velocity dispersion. For comparison, the bi-weight estimates (Beers, Flynn & Gebhardt 1990) for the systemic velocity and velocity dispersion are  $v_{r,bw} = -188.5 \pm 3.6 \text{ km s}^{-1}$  and  $\sigma_{bw} = 8.3 \pm 1.0 \text{ km s}^{-1}$ , respectively.

The large panel of Figure 2 shows the location of our seven program stars with respect to the center of And II. The

dashed lines show the major and minor axes of the galaxy, where we have estimated a position angle of  $\theta_0 = 160 \pm 15^\circ$  for the major axis of the galaxy based on a visual inspection of Figure 2 of Caldwell et al. (1992). The ellipse indicates the geometric mean King-Michie core radius of  $r_c = 1'.86$  (see §3.2), where  $e \equiv 1 - b/a = 0.3$  (Caldwell et al. 1992). The seven stars having measured radial velocities are found in the same quadrant of the galaxy, although five of these objects lie within one core radius of the galaxy's center while the two remaining stars are located considerably further out, at radii of  $4'.65$  and  $6'.00$ .

In the upper and right panels of Figure 2, we plot the heliocentric radial velocities for the seven stars as a function of perpendicular distance from the major and minor axes, respectively. Interestingly, the two most distant stars both have radial velocities of  $v_r \gtrsim -180 \text{ km s}^{-1}$ , whereas the velocities of the five stars near the center of the galaxy fall in the range  $-197 \lesssim v_r \lesssim -188 \text{ km s}^{-1}$ . This fact, along with the galaxy's rather high ellipticity, suggests that rotation might, at least in part, be responsible for the high velocity dispersion measured for And II. Such a result would be surprising since only one Galactic dSph galaxy (Ursa Minor) is known to be rotating, and even in this case, the rotation is dynamically unimportant:  $v_{\text{rot},0}/\sigma_0 \sim 0.5$  (Hargreaves et al. 1994; Armandroff, Olszewski & Pryor 1995). In the next section, we discuss the possible effects of rotation on the derived mass-to-light ratio for And II.

#### 3.2. Mass-to-Light Ratio

We have estimated the mass-to-light ratio of And II in two different ways. First, we have fit an isotropic, single-mass King-Michie model to the  $V$ -band surface brightness profile given in Caldwell et al. (1992), assuming  $E(B - V) = 0.062 \text{ mag}$ ,  $A_V = 3.1E(B - V)$  and  $D = 660 \text{ kpc}$  (Côté et al. 1999b). The parameters of this model are given in Table 2, along with other fundamental parameters for And II. Both the radii used in the fit and those quoted in this table are geometric mean radii. The tabulated ( $1\sigma$ ) uncertainties in these parameters have been determined by fitting King-Michie models to each of 100 simulated data sets generated from the original model and using the uncertainties in the observed surface brightness profile (see Fischer et al. 1992). Integrating the isotropic model over all radii gives a total luminosity of  $L_V = (2.95_{-0.50}^{+0.73}) \times 10^6 L_{V,\odot}$  for And II. Based on the seven radial velocities given in Table 1, we find a scale velocity of  $v_s = 10.8_{-3.0}^{+3.1} \text{ km s}^{-1}$  and a systemic velocity of  $v_0 = -185.4 \pm 3.5 \text{ km s}^{-1}$  for this model. These values correspond to a central velocity dispersion of  $\sigma_0 = 9.3_{-2.6}^{+2.7} \text{ km s}^{-1}$  and  $M/L_V = 20.9_{-10.1}^{+13.9} M_\odot/L_{V,\odot}$ , which we adopt as our best estimate for the global mass-to-light ratio for And II. Note that if the sample is limited to just the five stars with  $r < r_c$ , this estimate drops to  $M/L_V = 2.0_{-1.3}^{+1.9} M_\odot/L_{V,\odot}$ , demonstrating that the high mass-to-light ratio found here is due to the large velocity residuals of the two outermost stars.

As a check on the above mass-to-light ratio, we have also used the tensor virial theorem to estimate the mass of And II, explicitly including the possible effects of rotation. Naturally, with a sample of only seven radial velocities,

<sup>6</sup>IRAF is distributed by the National Optical Astronomy Observatories, which are operated by the Association of Universities for Research in Astronomy, Inc., under contract to the National Science Foundation.

the exact form of the rotation law (if any) is hopelessly under-constrained. Our goal here is simply to explore the possible effects of ordered motions on the inferred velocity dispersion and, hence, on the derived mass-to-light ratio. In the right and upper panels of Figure 2 we show the rotation-corrected velocities for the seven And II members assuming that, over the region spanned by these stars, the galaxy is rotating as a solid-body about the minor and major axes, respectively. The virial mass is then given by

$$M = \frac{2\bar{r}}{G}(v_{\text{rot},0}^2 + 3\sigma_0^2) \quad (2)$$

where  $v_{\text{rot},0}$  is the mass-weighted rotation velocity,  $\sigma_0$  is the mass-weighted velocity dispersion and  $\bar{r}$  is the harmonic radius (*e.g.*, see Meylan & Mayor 1986). The rotation-corrected velocities (*i.e.*, the open circles in Figure 2) are then used to derive  $\sigma_0$ , approximating the density profile by the isotropic King model discussed above (which assumes that mass traces light). In the two cases of solid-body rotation about the major and minor axes, the derived mass-to-light ratios are  $M/L_V = 63$  and  $19M_\odot/L_{V,\odot}$ , respectively. If rotation is neglected (*i.e.*, the uncorrected velocities are used), then the virial mass estimator gives  $M/L_V = 22$ , in agreement with the preceding results.

### 3.3. Discussion

We now discuss the implications of the mass-to-light ratio of And II presented here, concentrating on three possible interpretations: (1) Modified Newtonian Dynamics (MOND); (2) non-equilibrium dynamics; and (3) dark matter.

#### 3.3.1. Modified Newtonian Dynamics

Milgrom (1983, 1995) has argued that dSph galaxies occupy a “low-acceleration regime” in which Newton’s second law deviates from the standard  $r^{-2}$  law. For isotropic velocity dispersion tensors, the MOND virial mass is given by

$$M = \frac{81}{4}\sigma_0^4(Ga_0)^{-1} \quad (3)$$

where  $G$  is the gravitational constant,  $\sigma_0$  is the central line-of-sight velocity dispersion and  $a_0 = 1.2 \times 10^{-8} \text{ cm s}^{-1}$  is the MOND acceleration constant. Adopting  $\sigma_0 = 9.3_{-2.6}^{+2.7} \text{ km s}^{-1}$  (the central velocity dispersion of the isotropic King-Michie model) and  $L_V = (2.95_{-0.50}^{+0.73}) \times 10^6 L_{V,\odot}$  gives  $M/L_V = 3.2_{-2.3}^{+4.8} M_\odot/L_{V,\odot}$  for the MOND mass-to-light ratio, which is consistent with the mass-to-light ratios of Galactic globular clusters. We conclude that MOND provides an adequate description of the internal kinematics of And II, without requiring the presence of a dark halo.

#### 3.3.2. Non-Equilibrium Dynamics: Tides

One possible explanation for the high central velocity dispersions of dSph galaxies is that these objects are not in dynamical equilibrium as a result of time-dependent oscillations caused by the tidal field of the host galaxy (*e.g.*, Kuhn & Miller 1989; Cuddeford & Miller 1990) or outright tidal disruption (Kroupa 1997; Klessen & Kroupa 1998).

Might this be the case for And II? Following Mateo et al. (1993), we calculate for each Local Group dE/dSph galaxy a “stability index”,  $X = \log_{10}(\rho_{V,0}/\rho_{\text{Gal}})$ , where  $\rho_{V,0} \sim \mu_{V,0}/2r_c$  is the central density of the dSph galaxy (determined from the observed surface brightness profile and an assumed mass-to-light ratio of  $M/L_V = 2M_\odot/L_{V,\odot}$ ) and  $\rho_{\text{Gal}}$  is the mean density of the host galaxy interior to the position of each satellite. The latter values have been calculated assuming logarithmic potentials for M31 and the Milky Way having circular velocities of  $v_c = 260$  and  $220 \text{ km s}^{-1}$ , respectively. The results of this exercise are shown in the upper panel of Figure 3. For And II, we find  $\rho_{V,0} = 0.012 \pm 0.003 M_\odot \text{ pc}^{-3}$  and  $X \sim 2.1$ , meaning that the internal baryonic mass density in And II is  $\sim 120$  times greater than the average enclosed mass density (*i.e.*, dark matter and baryons). Evidently, tides are unlikely to play an important role in driving the internal kinematics of And II.<sup>7</sup>

#### 3.3.3. Dark Matter

The lower panel of Figure 3 shows the global mass-to-light ratios of Local Group dE/dSph galaxies (data from Mateo 1998) plotted as a function of their absolute magnitude. Clearly, And II is consistent with the established trend between mass-to-light ratio and integrated luminosity (Kormendy 1987). In addition, the mass-to-light ratio found here is consistent, at the  $1.2\sigma$  level, with the suggestion (Mateo et al. 1993; Mateo 1998) that all dE/dSph galaxies studied to date consist of luminous components having  $M/L_V = 2M_\odot/L_{V,\odot}$  which are embedded in dark matter halos of mass  $M \sim 2 \times 10^7 M_\odot$ , as indicated by the dashed line in Figure 3.

The authors thank Phil Fischer for useful discussions, and the referee, Tad Pryor, for his prompt and helpful comments. PC acknowledges support provided by the Sherman M. Fairchild Foundation. MM was partially supported by grants from the NSF during the course of this research. EWO was partially supported by NSF grants AST 92-23967 and AST 96-19524.

<sup>7</sup>Although M33 is  $\sim 2\times$  nearer (in projection) to And II, its influence is negligible compared to that of M31 due to its much lower mass (*e.g.*,  $v_c \sim 80 \text{ km s}^{-1}$  according to Figure 3 of Zaritsky, Elston & Hill 1989).

TABLE 1  
 RADIAL VELOCITIES FOR RED GIANTS IN ANDROMEDA II

ID	$V$ (mag)	$(V - I)$ (mag)	$R$ (')	$\theta$ (deg)	HJD 2440000+	$R_{TD}$	$v_r$ (km s <sup>-1</sup> )	$\bar{v}_r$ (km s <sup>-1</sup> )
And II-5	21.89	1.72	1.36	243	11101.8579	3.97	-192.3±2.4	-192.6±1.6
					11101.9021	4.45	-192.8±2.2	
And II-32	21.82	1.81	0.72	221	11101.9499	5.05	-188.1±2.0	-188.1±2.0
And II-22	21.65	1.69	4.65	195	11101.9961	3.41	-180.1±2.7	-178.7±1.8
					11102.0407	4.05	-177.6±2.4	
And II-4	21.91	1.62	0.53	250	11102.7910	7.08	-188.9±1.5	-188.9±1.5
And II-11	21.94	1.63	1.61	200	11102.8367	4.97	-194.8±2.0	-194.8±2.0
And II-36	22.05	1.78	1.29	181	11102.9153	4.12	-197.3±2.3	-197.3±2.3
And II-26	21.82	1.66	6.00	191	11103.0083	4.11	-176.4±2.3	-176.4±2.3

TABLE 2  
OBSERVED AND DERIVED PARAMETERS FOR ANDROMEDA II

Quantity	Symbol	Value	Units	Reference
Distance	$D$	$660^{+100}_{-85}$	kpc	4
True Distance Modulus	$(m - M)_0$	$24.1 \pm 0.3$	mag	4
Reddening	$E(B - V)$	$0.062 \pm 0.010$	mag	3
Absolute Magnitude	$M_V$	$-11.40^{+0.23}_{-0.19}$	mag	2,5
Core Radius	$r_c$	$1.89^{+0.47}_{-0.37}$	arcmin	2,5
		$362^{+91}_{-71}$	pc	2,5
Half-Mass Radius	$r_h$	$3.27^{+1.12}_{-0.50}$	arcmin	2,5
		$627^{+216}_{-96}$	pc	2,5
Tidal Radius	$r_t$	$13.8^{+11.4}_{-4.5}$	arcmin	2,5
		$2.65^{+2.19}_{-0.86}$	kpc	2,5
Concentration	$c$	$0.87^{+0.37}_{-0.25}$		2,5
Ellipticity	$e$	0.3		2
Position Angle	$\theta_0$	$160 \pm 15$	deg	2,5
Central Surface Brightness	$\mu_{V,0}$	$24.75 \pm 0.12$	mag arcsec <sup>-2</sup>	2,5
		$4.43^{+0.50}_{-0.47}$	$L_{V,\odot} \text{ pc}^{-2}$	2,5
Integrated Luminosity	$L_V$	$(2.95^{+0.73}_{-0.50}) \times 10^6$	$L_{V,\odot}$	2,5
Maximum Likelihood Mean Velocity	$v_0$	$-188.1 \pm 2.8$	km s <sup>-1</sup>	5
Biweight Central Velocity	$v_{r,bw}$	$-188.5 \pm 3.6$	km s <sup>-1</sup>	5
Maximum Likelihood Dispersion	$\sigma_{mle}$	$7.1 \pm 2.1$	km s <sup>-1</sup>	5
Biweight Velocity Dispersion	$\sigma_{bw}$	$8.3 \pm 1.0$	km s <sup>-1</sup>	5
<i>King-Michie Model</i>				
Scale Velocity	$v_s$	$10.8^{+3.1}_{-3.0}$	km s <sup>-1</sup>	5
Central Velocity Dispersion	$\sigma_0$	$9.3^{+2.7}_{-2.6}$	km s <sup>-1</sup>	5
Mass-to-Light Ratio	$M/L_V$	$20.9^{+13.9}_{-10.1}$	$M_\odot/L_{V,\odot}$	5
Mass-to-Light Ratio ( $r < r_c$ , $N_* = 5$ )		$2.0^{+1.9}_{-1.3}$	$M_\odot/L_{V,\odot}$	5
<i>Virial Theorem</i>				
Mass-to-Light Ratio (no rotation)		22	$M_\odot/L_{V,\odot}$	5
Mass-to-Light Ratio (minor axis rotation) <sup>a</sup>		19	$M_\odot/L_{V,\odot}$	5
Mass-to-Light Ratio (major axis rotation) <sup>b</sup>		63	$M_\odot/L_{V,\odot}$	5

References for Table 2: (1) König et al. (1993); (2) Caldwell et al. (1992); (3) Schlegel, Finkbeiner & Davis (1998); (4) Côté, Oke & Cohen (1999b); (5) This paper

<sup>a</sup>Mass-to-light ratio found using radial velocities corrected for solid-body rotation around the galaxy's minor axis (*e.g.*, see the right panel of Figure 2).

<sup>b</sup>Mass-to-light ratio found using radial velocities corrected for solid-body rotation around the galaxy's major axis (*e.g.*, see the upper panel of Figure 2).

## REFERENCES

- Aaronson, M. 1983, *ApJ*, 266, L11  
 Aaronson, M., Olszewski, E., Gordon, G.D, Mould, J.R., & Suntzeff, N. 1985, *ApJ*, 296, L7  
 Armandroff, T.E., Olszewski, E.W., & Pryor, C. 1995, *AJ*, 110, 2131  
 Armandroff, T.E., Davies, J.E., & Jacoby, G.H.  
 Beers, T.C., Flynn, K., & Gebhardt, K. 1990, *AJ*, 100, 32  
 Binney, J. & Tremaine, S. 1987, *Galactic Dynamics*, (Princeton, Princeton University Press)  
 Caldwell, N., Armandroff, T.E., Seitzer, P., & Da Costa, G.S. 1992, *AJ*, 103, 840  
 Caldwell, N., Armandroff, T.E., Da Costa, G.S. & Seitzer, P. 1998, *AJ*, 115, 535  
 Cook, K., Mateo, M., Olszewski, E.W., Vogt, S.S., Stubbs, C., & Diercks, A. 1999, *PASP*, 111, 306  
 Côté, P., Djorgovski, S.G., Meylan, G., & McCarthy, J.K. 1999a, in preparation  
 Côté, P., Oke, J.B., & Cohen, J.C. 1999b, *AJ*, in press  
 Cuddeford, P., & Miller, J.C. 1990, *MNRAS*, 244, 64  
 Fischer, P., Welch, D.L., Mateo, M., Côté, P., & Madore, B.F. 1992, *AJ*, 103, 857  
 Hargreaves, J.C., Gilmore, G., Irwin, M.J., & Carter, D. 1994, *MNRAS*, 271, 693  
 Hargreaves, J.C., Gilmore, G., & Annan, J.D. 1996, *MNRAS*, 279, 108  
 Klessen, R.S., & Kroupa, P. 1998, *ApJ*, 498, 143  
 König, C.H.B., Nemec, J.M., Mould, J.R., & Fahlman, G.G. 1993, *AJ*, 106, 1819  
 Kormendy, J. 1987, in *Dark Matter in the Universe*, ed. J. Kormendy and G. Knapp (Reidel, Dordrecht), 139  
 Kroupa, P. 1997, *New Astron.*, 2, 139  
 Kuhn, J.R., & Miller, R.H. 1989, *ApJ*, 341, L41  
 Mateo, M. 1998, *ARA&A*, 36, 435  
 Mateo, M., Olszewski, E.W., Pryor, C., Welch, D.L., & Fischer, P. 1993, *AJ*, 105, 510  
 Mateo, M., Olszewski, E.W., Voght, S.S., & Keane, M.J. 1998, *AJ*, 116, 2315  
 Milgrom, M. 1983, *ApJ*, 270, 365  
 Milgrom, M. 1995, *ApJ*, 455, 439  
 Meylan, G., & Mayor, M. 1986, *A&A*, 166, 122  
 Olszewski, E.W., Aaronson, M., & Hill, J.M. 1995, *AJ*, 110, 2120  
 Piatek, S., & Pryor, C. 1995, *AJ*, 109, 1071  
 Pryor, C., & Kormendy, J. 1990, *AJ*, 100, 127  
 Pryor, C., & Meylan, G. 1993, in *The Structure and Dynamics of Globular Clusters*, ed. S.G. Djorgovski & G. Meylan (San Francisco: ASP), 357  
 Suntzeff, N.B., Mateo, M., Terndrup, D.M., Olszewski, E.W., Geisler, D., & Weller, W. 1993, *ApJ*, 418, 208  
 Tonry, J., & Davis, M., 1979, *AJ*, 82, 954  
 van den Bergh, S. 1972, *ApJ*, 171, L31  
 Vogt, S.S., et al. 1994, *SPIE*, 2198, 362  
 Vogt, S.S., Mateo, M., Olszewski, E.W., & Keane, M.J. 1995, *AJ*, 109, 151  
 Zaritsky, D., Elston, R., & Hill, J.M. 1989, *AJ*, 97, 97

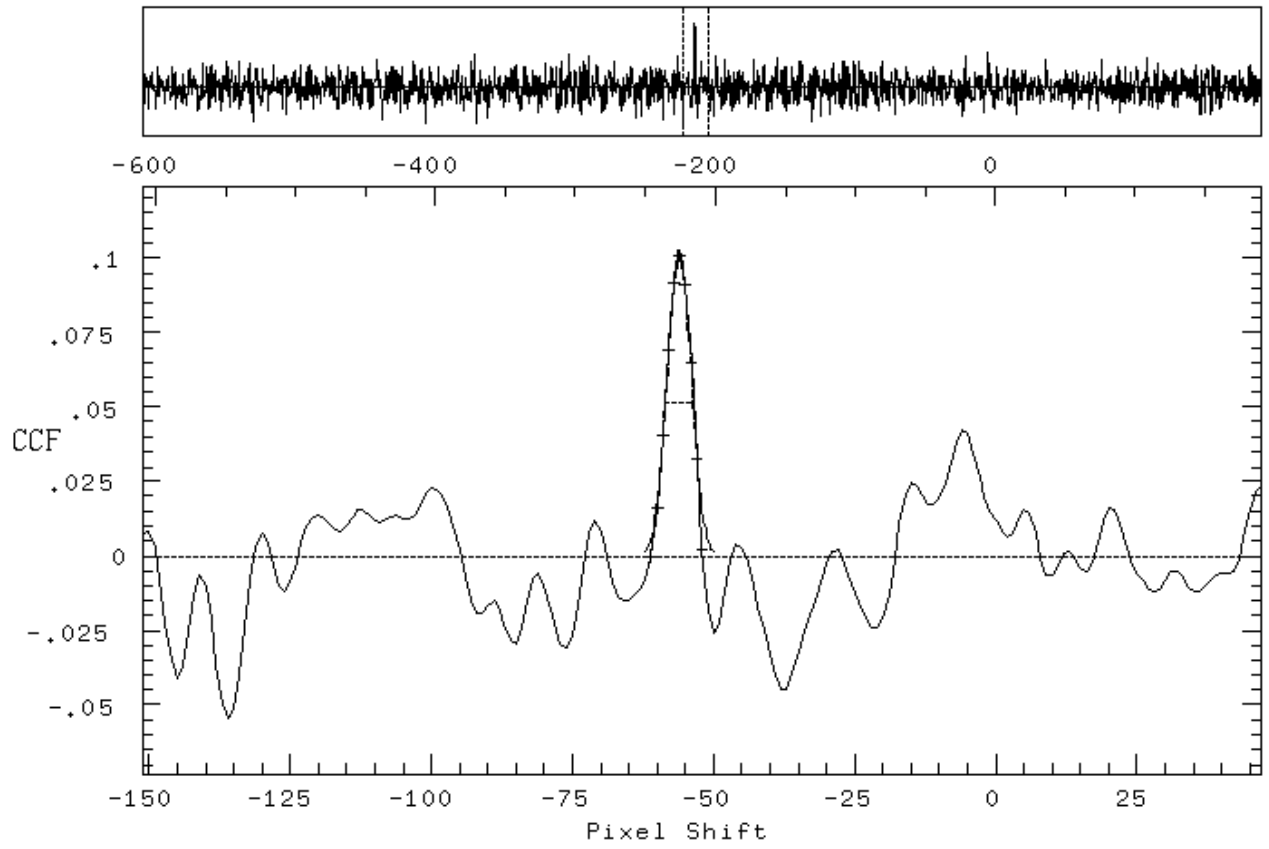


FIG. 1.— Cross-correlation function for Andromeda II-5 obtained using our master radial velocity template. The Tonry-Davis  $R_{TD}$  value for this cross correlation is  $R_{TD} = 4.45$ , slightly lower than the average of  $\overline{R_{TD}} = 4.58$  for the nine measurements given in Table 1.

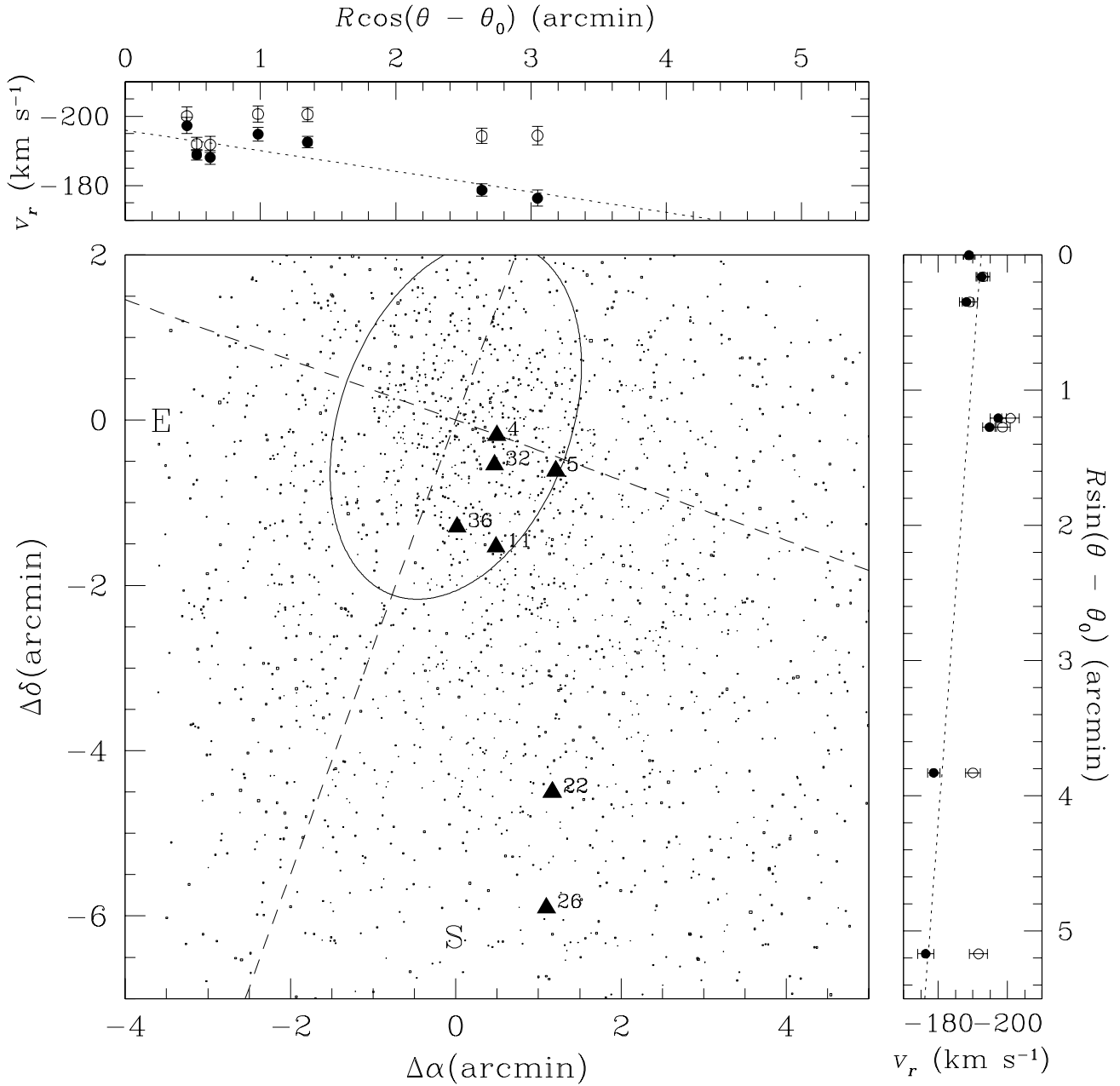


FIG. 2.— (Large Panel) Distribution of unresolved objects in the vicinity of Andromeda II. Red giants having one or more measured radial velocities are indicated by the large triangles. The core radius of Andromeda II is indicated by the ellipse, which has  $r_c = 1'89$ ,  $a = 2'26$  and  $b/a = 0.7$  (Caldwell et al. 1992). The dashed lines indicate the minor and major axes of the galaxy. (Upper Panel) Radial velocities for Andromeda II members plotted against distance along the photometric minor axis (filled circles). The dotted-line indicates the weighted least-squares fit to the points. The open circles show the rotation-corrected velocities, assuming solid-body rotation about the *major* axis. (Right Panel) Same as previous panel, except for the case of solid-body rotation about the photometric *minor* axis.

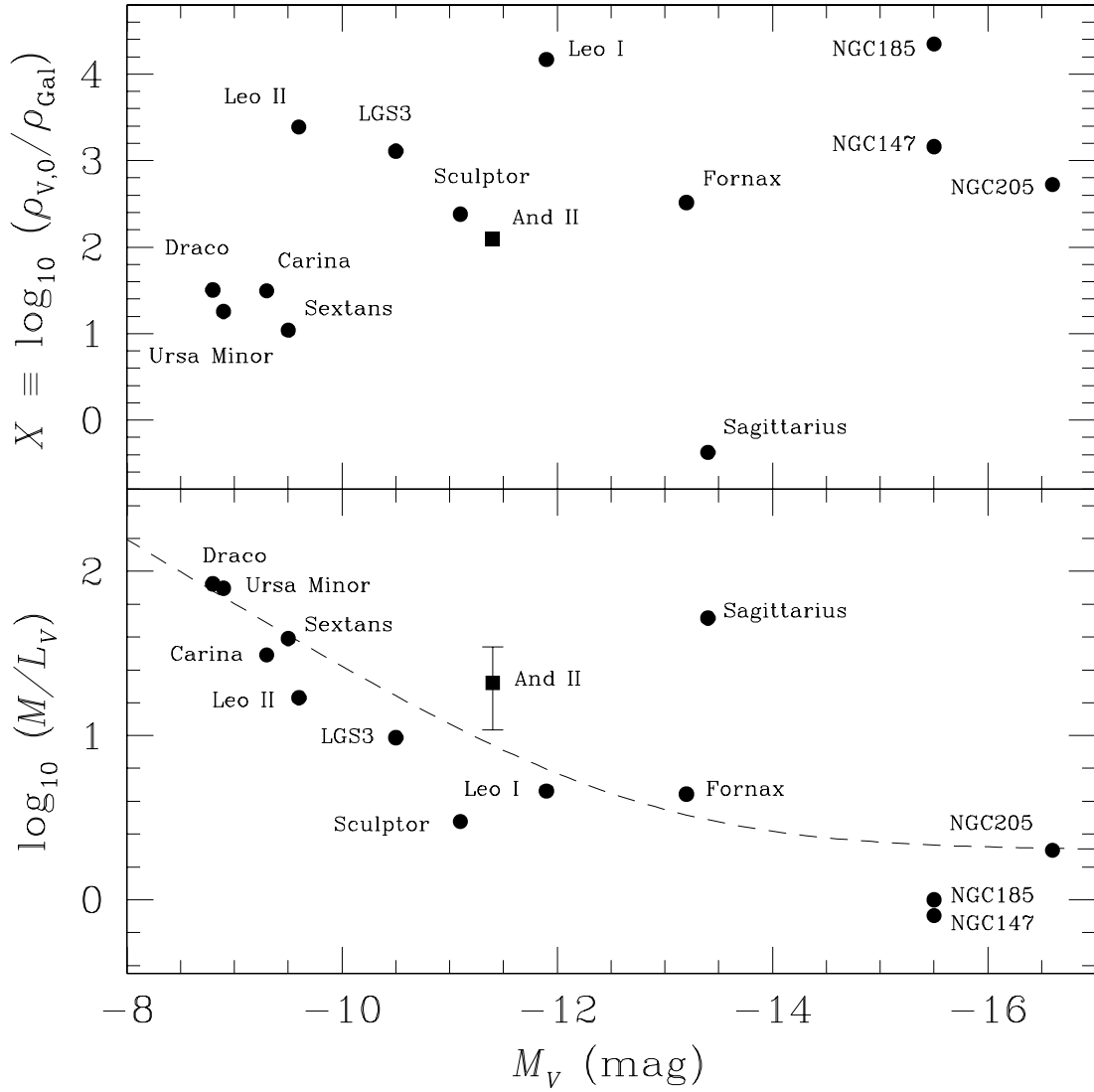


FIG. 3.— (Upper Panel) Stability index,  $X$ , for Local Group dE/dSph galaxies plotted against  $V$ -band absolute magnitude (circles). The total of the Milky Way is assumed to be  $1 \times 10^{12} M_{\odot}$ . The mass of M31 is taken to be twice this value. (Lower Panel) Global  $V$ -band mass-to-light ratio for Local Group dE/dSph galaxies, plotted against  $V$ -band absolute magnitude (circles). The dashed line indicates the expected relation for dwarfs consisting of luminous components having  $M/L_V = 2M_{\odot}/L_{V,\odot}$  which are embedded in dark matter halos of mass  $M \sim 2 \times 10^7 M_{\odot}$ .